International Science and Technology Journal
المجلة الدولية للعلوم والتقنية
Volume 33 العدد
Part 1 المجلد
October 2023 اكتوبر
المجلة الدولية للعلوم والتقنية
ISTJ
تم استلام الورقة بتاريخ:24/ 8 /2023م وتم نشرها على الموقع بتاريخ:1/ 10/2023م

Simplified Numerical Model of Wind Loads on Suspension Transmission Towers Using CFD and Static Structure Package

Akram Abdullah Alharari, [a] Abdulmajed Abuajela A Khalifa, Mohammed Mosbah Alfaqeeh,Alhosain Taher Abdelhameed

Mechanical Engineering Department, Faculty of Engineering,
University of Zawia, Libya.
[a] a.khaliefa@zu.edu.ly

Abstract

In this paper, the effect of wind pressure on the electrical transmission tower structure was numerically simulated and analyzed. The numerical model was built based on existing towers used in Libya, scaled down by the scale of 1:10. The wind pressure was obtained from a CFD simulation of the wind flow over the tower using ANSYS Fluent. Then, the stresses and deformations of the towers, which resulted from the wind pressure, were calculated using ANSYS Static Structure program. There sults showed that wind velocity and pressures exerted by the wind share an exponential relationship, where a slight increase in wind velocity leads to a significant increase in pressure exerted on the tower. The total deformation and equivalent stresses have a linear relationship with the wind pressure and an exponential relationship with the wind velocity.

Keywords: Suspension Tower design, Finite element analysis, ANSYS, static analysis, CFD simulation

International Science and Technology Journal
المجلة الدولية للعلوم والتقنية
Volume 33 العدد
Part 1 المجلد
October 2023 اكتوبر
المجلة الدولية للعلوم والتقنية
ISTJ
تم استلام الورقة بتاريخ:24/ 8 /2023م وتم نشرها على الموقع بتاريخ:1/ 10/ 2023م

نموذج رقمي مبسط لتأثير الرياح على أبراج نقل الطاقة الكهربائية باستخدام CFD و Static Structure

اكرم عبد الله الحراري, عبد المجيد ابوعجيلة خليفة,
محمد مصباح الفقيه, الحسين طاهر عبد الحميد
قسم الهندسة الميكانيكية والصناعية, كلية الهندسة, جامعة الزاوية

الملخص

تم في هذا البحث تحليل تأثير ضغط الرياح على هياكل أبراج نقل الطاقة الكهربائية باستخدام طرق التحليل العددي. النموذج العددي المستخدم يحاكي الأبراج الموجودة والمستخدمة في ليبيا ولكن تم تصغير حجمها بمقياس 1 إلى 10. في الخطوة الأولى تم حساب قوة ضغط الرياح المؤثرة على الأبراج وذلك باستخدام ANSYS Fluent ومن ثم تم حساب الإجهادات والتشوهات الناتجة عن ضغط الرياح باستخدام برنامج ANSYS Static Structure. أظهرت النتائج أن سرعة الرياح والضغوط الناتجة عنها ترتبط بعلاقة لوغاريتمية، حيث تؤدي الزيادة الطفيفة في سرعة الرياح إلى زيادة كبيرة في الضغط المسلط على البرج. وكذلك وجد ان التشوهات الكلية والضغوط المكافئة لها تتغير خطيا مع ضغط الرياح ولوغاريتميا مع سرعة الرياح.

الكلمات المفتاحية: تصميم البرج المعلق، تحليل العناصر المحدودة، ANSYS، التحليل الساكن، محاكاة CFD

1. Introduction

Wind loading is one of the primary horizontal loads acting on towers, and its appropriate consideration is necessary to satisfy the design requirements. The static and dynamic wind effects are also important, particularly for suspension towers, which may induce significant vibrations not only along wind direction but also in the vertical and torsional directions. These effects must be circumvented or reduced to acceptable magnitudes. The wind loading on the towers will result in uplift or compression forces transmitted through the tower legs to the foundations. Terminal or

تم استلام الورقة بتاريخ:24/ 8 /2023م وتم نشرها على الموقع بتاريخ:1/ 10/2023م

heavy-angle towers will have tower leg foundations remaining in uplift or compression although a check is necessary to ensure broken wire conditions do not reverse the effect. Straight-line or light-angle towers can have the loading reversed depending upon the wind direction and therefore the foundations for each tower leg must be capable of restraint in both modes. Several studies have analyzed and designed transmission towers, ranging from experimental wind tunnel studies to finite element analyses of the structural performance of the tower. When modeling wind loads, the wind load is treated as a dynamic load, especially in the academic research fields; however, for practical design and engineering of the towers, the wind is treated as a static load for simplification. This is seen in Australian and United States standards, where conditions such as terrain properties, topography, and the direction the wind is travelling in order to determine the wind speed and consequently convert the speed into wind pressure on the tower [1-4]. Many researchers have implemented this method of simplification such as a study by Panwar et al. who used it for structural analysis and design of steel transmission used in India [5], a study by Chyrmang, who studied typical type of transmission line towers carrying 400kV double circuit conductor [6], and a study by Pal et al. which studied a 220 KV suspension type, and square-based self-supporting transmission tower with double circuits [7]. The present study is based on previously unpublished work conducted by the Authors in 2019 as part of the student's final year project in the mechanical engineering department, university of Zawia. The CFD simulation of air passing through the tower was used to calculate the pressure exerted on the steel lattices instead of static load calculations, which will determine the stresses and deformations resulting from this load.

2.Physical Model

Figure 1 illustrates a simplified model of a power transmission line that was implemented in this study. The tower was scaled down ten times (1:10 scale) compared to the original transmission tower available in Libya with the main dimensions shown in Figure 1. This simplification was made to keep the mesh and the computational

تم استلام الورقة بتاريخ:24/ 8 /2023م وتم نشرها على الموقع بتاريخ:1/ 10/2023م

time within the allowed size of the student version of the ANSYS program.

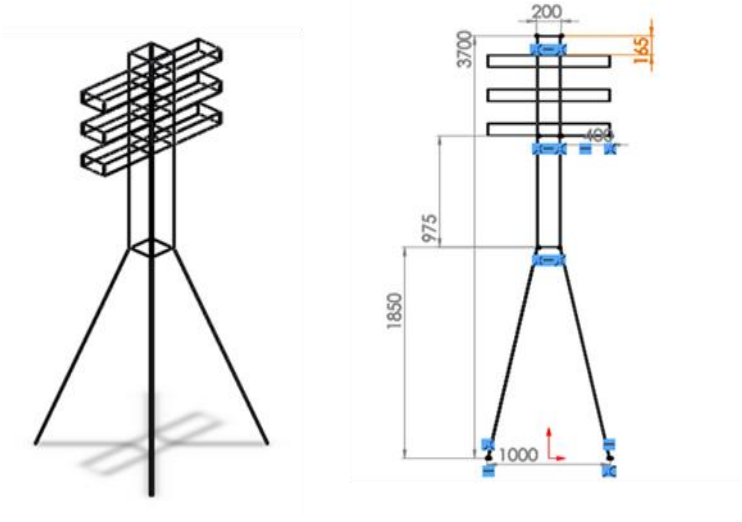

Figure 1. Tower design after simplification (dimensions in mm)

Consequently, the model is not expected to give an accurate representation of the wind loads on the transmission towers; however, it should provide a general idea of their effect. As seen in Figure 2, in the CFD simulation an enclosure was created surrounding the tower to represent the wind flow around the tower.

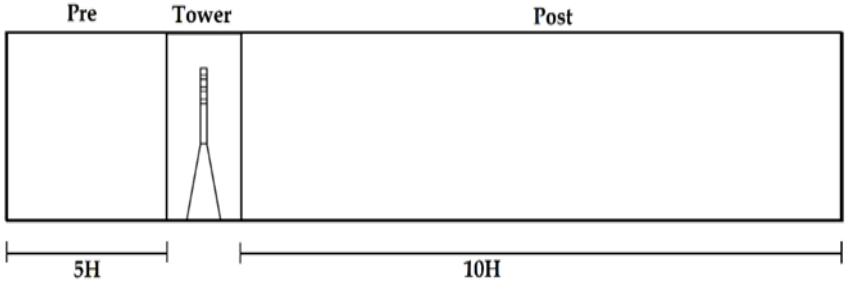

Figure 2.The model used in CFD analysis

تم استلام الورقة بتاريخ:24/ 8 /2023م وتم نشرها على الموقع بتاريخ:1/ 10/2023م

A safe distance was made before the tower, five times the tower height, to ensure that the airflow is fully developed once it reaches the tower. A safe distance was also made after the tower, to ensure that the wake effect due to the air passing through the tower was properly observed as well as to avoid any instability in convergence during the simulation. The CFD simulation will be modelled and conducted using ANSYS fluent V15.0.7 commercial software [8]. The tower is made of structure steel [9] with physical properties shown in Table 1.

Table 1. Physical properties of structural steel

Density	7850 kg/m^3
Compressive and tensile Yield Strength	250Mpa
Tensile Ultimate Strength	460Mpa
Young's Modulus	200GPa
Poisson's Ratio	0.3
Bulk Modulus	167GPa
Shear Modulus	**76.9GPa**

3.The assumptions used in the simulation model

In order to simplify the problem and improve convergence, numerous assumptions were made. The main assumptions made in this study include:

For CFD analysis:

a. All walls are stationary and impermeable.
b. Gravity is neglected.
c. The flow is three-dimensional, turbulent and steady state.
d. All material properties are assumed to be constant, homogenous and isotropic.
e. The fluid is assumed to be Newtonian and incompressible.
f. Body forces and buoyancy effects are neglected.

For structure analysis:

a. No time-varying loads applied.
b. The load is static.
c. No internal stresses before loading.
d. Accelerations equal zero.

تم استلام الورقة بتاريخ:24/ 8 /2023م وتم نشرها على الموقع بتاريخ:1/ 10/2023م

e. Steady loading and response conditions are assumed; that is, the loads and the structure's response are assumed to vary slowly with respect to time.

4.Fluent model boundary conditions

The boundary conditions implemented in this study consist of velocity inlet, pressure outlet, and no-slip condition at the bottom of the domain, representing the ground and the tower's walls. The rest of the domain was set to shear-less walls to represent the open-air areas. Figure 3 illustrates the frontal and side views of the domain and the boundary conditions applied. The velocities used range from 0.25-4m/s, corresponding to 2.5-40m/s on a full-scale tower.

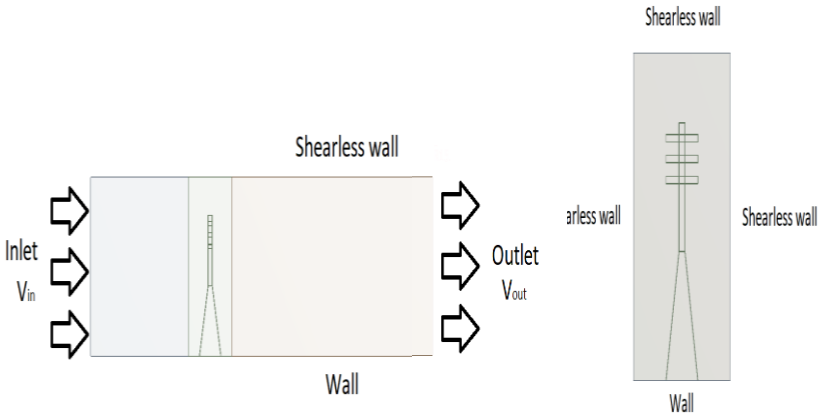

Figure 3. Boundary conditions for the frontal and side view of the CFD model

5.Fluent model solution method

The turbulent three-dimensional steady-state model was solved by ANSYS Fluent. The conservation equations of mass, momentum, and energy were solved using a second-order up wind discretization scheme to improve accuracy, while the standard k-ε turbulent model was solved using a first-order scheme to improve stability. The pressure-velocity coupling scheme followed the SIMPLE algorithm was adopted as recommended by Patanker [10] and it is summarized below:

تم استلام الورقة بتاريخ:24/ 8 /2023م وتم نشرها على الموقع بتاريخ:1/ 10/2023م

$$\left(\frac{\partial u}{\partial x}\right)+\left(\frac{\partial v}{\partial y}\right)+\left(\frac{\partial w}{\partial z}\right)=0 \quad (1)$$

$$\rho\left(u\frac{\partial u}{\partial x}+v\frac{\partial u}{\partial y}+w\frac{\partial u}{\partial z}\right) = -\frac{\partial p}{\partial x}+\rho g_x+\mu\left(\frac{\partial^2 u}{\partial x^2}+\frac{\partial^2 u}{\partial y^2}+w\frac{\partial^2 u}{\partial z^2}\right) \quad (2)$$

$$\rho\left(u\frac{\partial v}{\partial x}+v\frac{\partial v}{\partial y}+w\frac{\partial v}{\partial z}\right) = -\frac{\partial p}{\partial y}+\rho g_y+\mu\left(\frac{\partial^2 v}{\partial x^2}+\frac{\partial^2 v}{\partial y^2}+w\frac{\partial^2 v}{\partial z^2}\right) \quad (3)$$

$$\rho\left(u\frac{\partial w}{\partial x}+v\frac{\partial w}{\partial y}+w\frac{\partial w}{\partial z}\right)=-\frac{\partial p}{\partial z}+\rho g_z+\mu\left(\frac{\partial^2 w}{\partial x^2}+\frac{\partial^2 w}{\partial y^2}+w\frac{\partial^2 w}{\partial z^2}\right) \quad (4)$$

$$\frac{\partial}{\partial x_i}(\rho k u_i)=\frac{\partial}{\partial x_j}\left[\left(\mu+\frac{\mu_t}{\sigma_k}\right)\frac{\partial k}{\partial x_j}\right]+P_k-\rho\varepsilon \quad (5)$$

Where u, v and w represent the velocity components,ρ the fluid's density, P is the pressure, g is the gravidity, $\mu$is the fluid's viscosity, and ε represents the turbulent dissipation.

6.Static structure boundary conditions and parameters

The static boundary conditions implemented are the constant pressure induced by the wind on the tower's beams and the tower's weight applied on the tower's feet. The pressure is automatically imported and distributed from the previous calculation done via ANSYS Fluent to reflect the actual wind pressure and distribution. The value of this pressure differs based on the location and the wind velocity. The maximum pressure of each wind velocity will be discussed later in the results section. Figure 4 illustrates the distribution of air pressure on the tower beams as imported from Fluent. The solution parameters involved structural parameters such as the total deformation and the equivalent stress (Von Mises Stress).

International Science and Technology Journal
المجلة الدولية للعلوم والتقنية
Volume 33 العدد
Part 1 المجلد
October 2023 اكتوبر
المجلة الدولية للعلوم والتقنية
ISTJ
تم استلام الورقة بتاريخ:24/ 8 /2023م وتم نشرها على الموقع بتاريخ:1/ 10/2023م

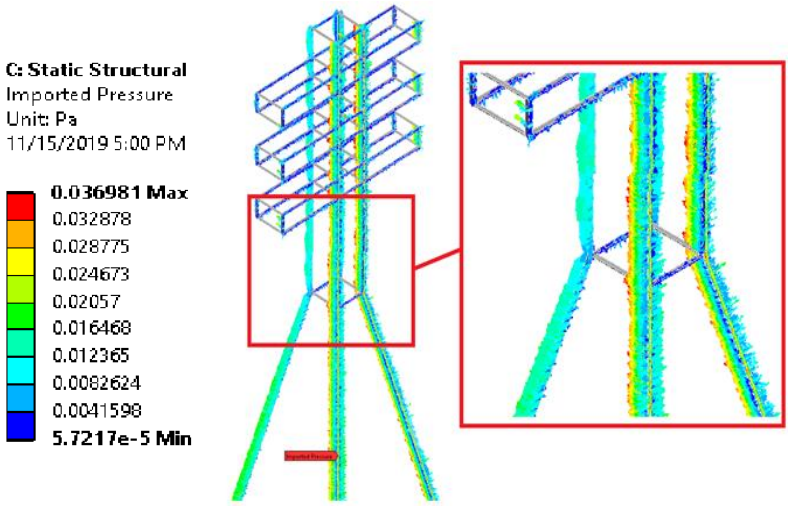

Figure 4. Imported pressure distribution from the CFD simulation

7.Static structure mathematical model

A static analysis was used to calculate the effects of steady loading conditions on the tower structure while ignoring inertia and damping effects, such as those caused by time-varying loads. However, the model includes some time-varying loads that can be approximated as static equivalent loads such as the static equivalent wind and seismic loads. The main equations used are as below:

$$W_{tower} = m_{tower} \times g \tag{6}$$

$$U_{total} = \sqrt{U_x + U_y + U_z} \tag{7}$$

$$\sigma_e = \sqrt{\frac{(\sigma_1 - \sigma_2)^2 + (\sigma_2 - \sigma_3)^2 + (\sigma_3 - \sigma_1)^2}{2}} \tag{8}$$

Where W_{tower} represents the tower's weight, $M_{tower}$is the tower's mass, $U_x, U_y, U_z$are the deformation components, and σ_e represents the equivalent von mises stress.

تم استلام الورقة بتاريخ:24/ 8 /2023م وتم نشرها على الموقع بتاريخ:1/ 10/2023م

8. Mesh

Figure 5 shows the adopted mesh in the simulation. As can be seen, the mesh was made smaller near the tower's walls, to ensure accuracy, compared to the other zones of the calculation domain. The overall number of elements and nodes used in this study is 2047742 elements and 352807 nodes. Similarly, the maximum cell skewness was 86%, which is lower than the maximum allowable skewness of 95% [1], and the average cell skewness was 24.12%. On the other hand, the average cell orthogonal quality was 85.29% and the highest was 99.69%.

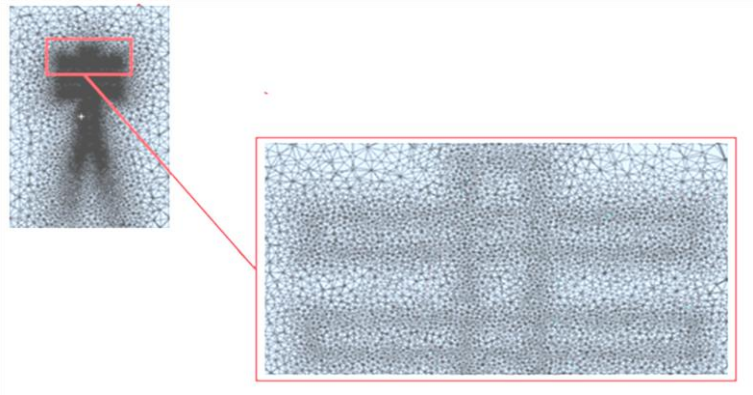

Figure 5.The mesh used in the study

9.Results

The results gained from the CFD simulation have shown a strong similarity between them and the turbulences generally found in the wake flow section of such towers. Wind velocity contours of 0.25m/s and 4m/s will be used throughout the remainder of this article. However, before presenting these results, the convergence history will be provided to illustrate the stability of the simulation and the accuracy of the solution.

9.1.Convergence History

The convergence history for wind velocities of 0.25m/s is shown in Figure 6. As can be seen, the convergence of the solution was achieved with reasonable stability and accuracy, where the convergence criteria chosen was 1.5×10^{-3}.

تم استلام الورقة بتاريخ:24/ 8 /2023م وتم نشرها على الموقع بتاريخ:1/ 10/2023م

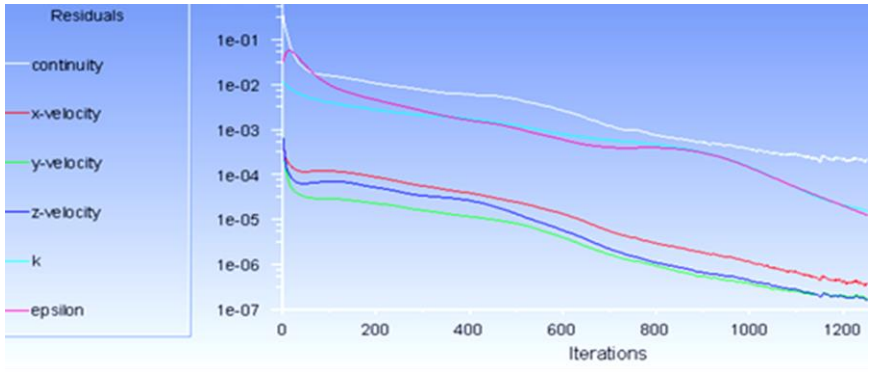

Figure 6. Convergence history for a wind velocity of 0.25m/s

9.2.Effect of Wind Velocity

As the air travels towards the tower, it is obstructed by the tower's steel lattices, which forces the air to circumvent these lattices resulting in a disparity in the pressure exerted on the tower lattices. The center of the steel lattice experiences higher pressure than its edges, as can be observed from the pressure contours shown in Figure7.

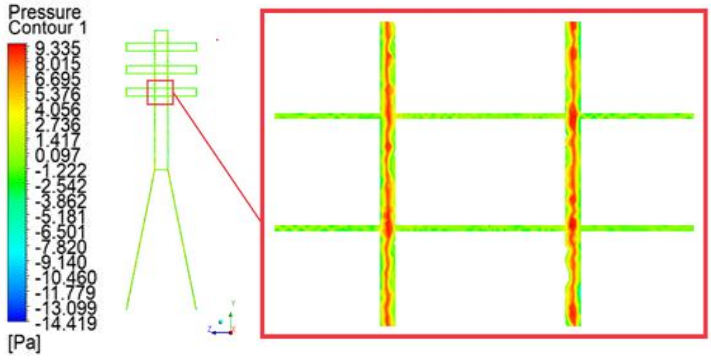

Figure 7. Sample of the pressure distribution across the tower's lattices.

9.3.Velocity Contour

Figures 8 and 9 illustrate the velocity contours at the mid-section of the tower from (a) the side view and (b) the top view at wind

تم استلام الورقة بتاريخ:24/ 8 /2023م وتم نشرها على الموقع بتاريخ:1/ 10/2023م

velocities of 0.25m/s and 4/m/s. It is apparently clear from the figures that the tower has a massive effect on the airflow with strong turbulences downstream, which is known as the wake effect. Once the air passes through or circumvents the tower, the wake effect starts to diminish and the air starts to regain its original flow characteristics. That is, the turbulent flow is dissipated and returns to laminar flow. Overall, there is no significant difference in the velocity contours, apart from the flow in the wake area.

9.4.Static Structural Results

The maximum total deformation and the equivalent stress are presented in the following two subsections:

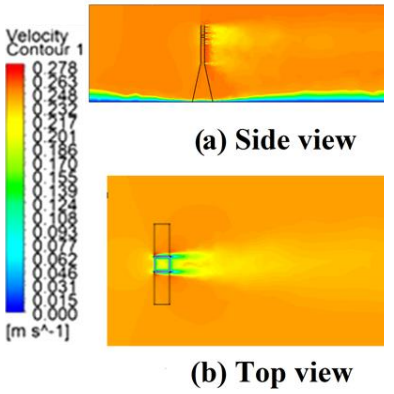

Figure 8. Velocity contours at the mid-section of the tower at a wind velocity of 0.25m/s

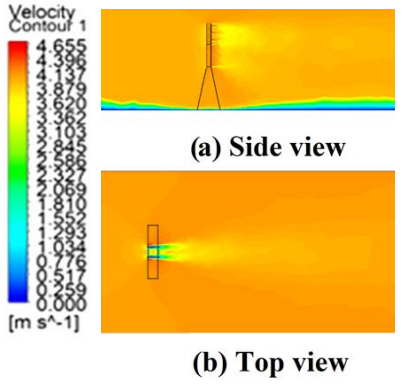

Figure 9. Velocity contours at the mid-section of the tower at a wind velocity of 4m/s

9.4.1.Total Deformation

Figures 10 and 11 show the relationship between the total deformation and the exerted wind pressure and velocity, respectively.

Furthermore, the total deformation contours for the top and bottom sections of the tower are presented in Figures 12 and 13.

تم استلام الورقة بتاريخ:24/ 8 /2023م وتم نشرها على الموقع بتاريخ:1/ 10/2023م

Where, the locations of maximum deformation are highlighted for wind velocities of 0.25m/s and 4m/s respectively. As these figures show, the highest deformation occurs at the mid-section of the tower's "legs" and the edges of the tower's "arms". This is expected since the weight of the top half of the tower places an extra burden on the tower's legs and the edges of the arms are the furthest part from the tower's body, which makes it more susceptible to the wind load and therefore more susceptible to deformation.

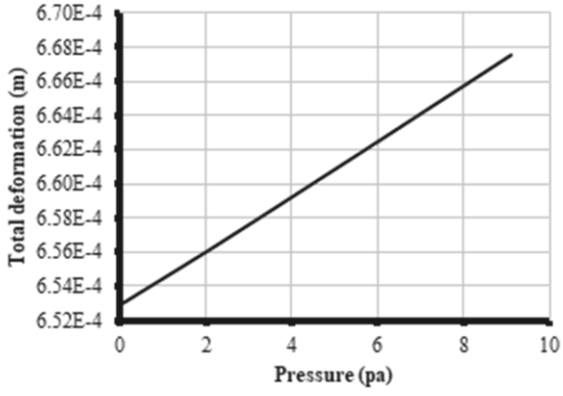

Figure 10.Effect of wind pressure on the deformation.

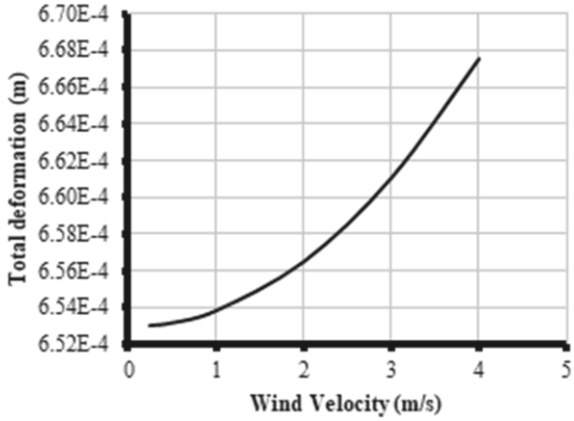

Figure 11. Effect of wind velocity on the deformation.

International Science and Technology Journal
المجلة الدولية للعلوم والتقنية
Volume 33 العدد
Part 1 المجلد
October 2023 اكتوبر
المجلة الدولية للعلوم والتقنية
ISTJ
تم استلام الورقة بتاريخ:24/ 8 /2023م وتم نشرها على الموقع بتاريخ:1/ 10/2023م

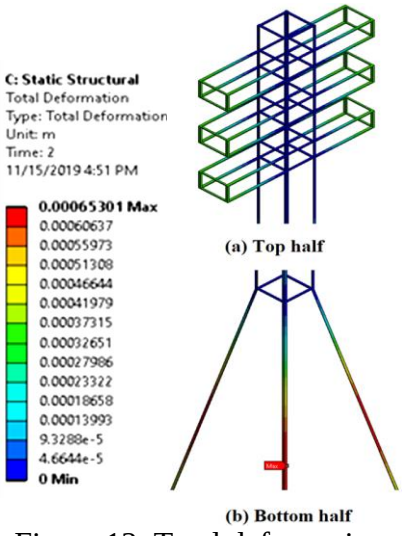

Figure 12. Total deformation for top and bottom sections of the tower for wind velocity 0.25m/s.

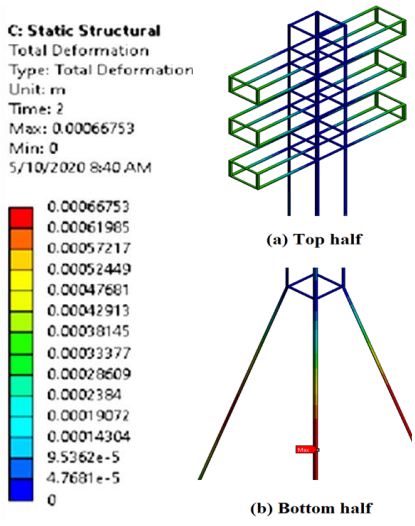

Figure 13. Total deformation for top and bottom sections of the tower for wind velocity of 4m/s.

9.4.2. Equivalent Stress

Correspondingly to the total deformation, the stresses resulting from the wind load have shown similar behavior, regardless of wind velocity. To keep the results of this study consistent, the same method used to portray the total deformation is used for the equivalent stress. That is, Figures 14 and 15 illustrate the effect of exerted wind pressure and wind velocity on the equivalent stress experienced by the tower. While there was no significant change in equivalent stress due to the increase in wind velocity from 0.25m/s to 0.5m/s, the equivalent stress has shown the same pattern as the total deformation. In other words, the equivalent stress increased in a linear manner with the exerted wind pressure and in an exponential manner with the wind velocity. To help illustrate the spread of these stresses across the tower, Figures 16 and 17 show the equivalent stress contours for the top and bottom sections of the tower and also indicate the locations of maximum and minimum stresses for wind velocities of 0.25m/s and 4m/s respectively. As these results indicate, the distribution of the stresses across the tower was

تم استلام الورقة بتاريخ:24/ 8 /2023م وتم نشرها على الموقع بتاريخ:1/ 10/2023م

extremely similar for both velocities. However, these stresses are concentrated at the arms of the tower, especially at both ends and at the lowest middle part of the arms. It should also be mentioned that despite slight stresses at the tower's fixed edges, there were no significant stresses at the tower's legs.

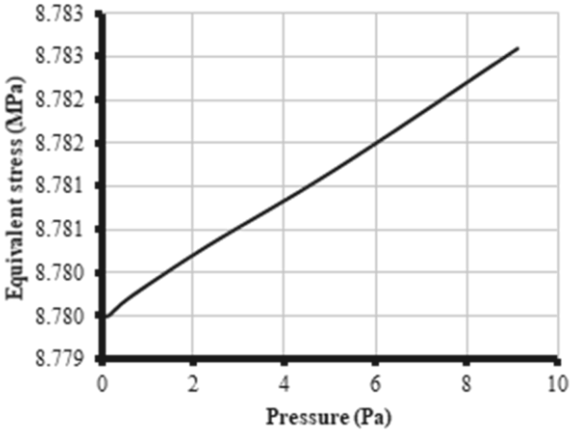

Figure 14. Effect of exerted wind pressure on the equivalent stress.

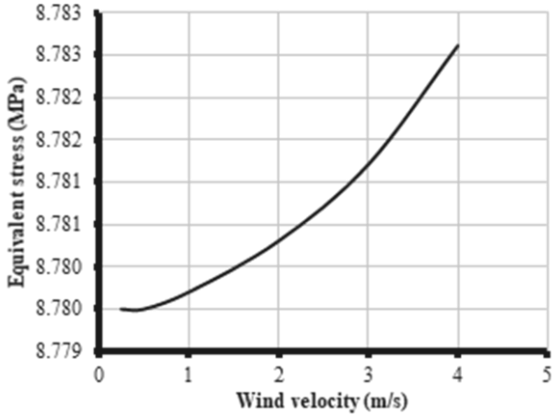

Figure 15. Effect of wind velocity on the equivalent stress.

تم استلام الورقة بتاريخ:24/ 8 /2023م وتم نشرها على الموقع بتاريخ:1/ 10/2023م

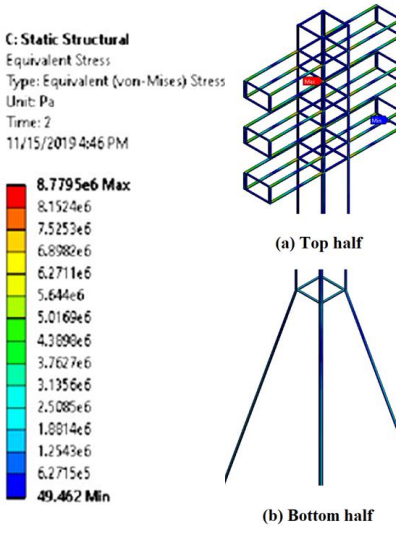

Figure 16. Equivalent stress contours for top and bottom sections of the tower for wind velocity of 0.25m/s.

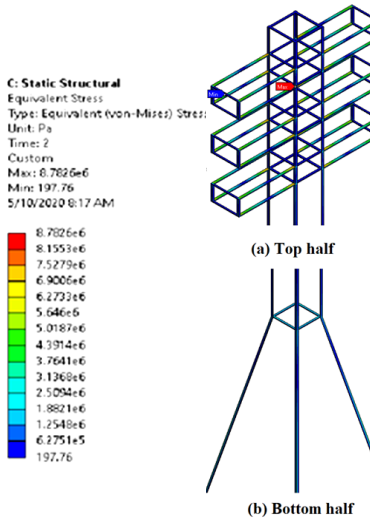

Figure 17. Equivalent stress contours for top and bottom sections of the tower for wind velocity of 4m/s.

10. Conclusion

Based on the results gained from this model, there are multiple conclusions that can be made, which are:

I. The wind velocity and pressure exerted by this wind share an exponential relationship, where an increase in wind velocity leads to a significant increase in pressure exerted by this wind.

II. Both the total deformation and the equivalent stress have a linear relationship with the exerted wind pressure and an exponential relationship with the wind velocity.

III. The distribution of the total deformation and equivalent stress due to the wind load remained fairly similar despite the increase in wind load.

IV. The ability to transfer forces and pressure from ANSYS Fluent to ANSYS static structure can help improve the accuracy of simulations that delve into the stresses caused by a flowing fluid inside or outside of solid objects as opposed to using static forces that may not reflect the actual behavior of fluids.

تم استلام الورقة بتاريخ:24/ 8 /2023م وتم نشرها على الموقع بتاريخ:1/ 10/2023م

11. References

[1] American Society of Civil Engineers (2009) ASCE Manual 74, Guidelines for electrical transmission line structural loading, ASCE, New York.

[2] Standards Australia (1994) AS 3995-1994, Design of steel lattice towers and masts, Standards Australia, NSW.

[3] American Society of Civil Engineers (2009) ASCE Manual 7, Minimun Design Loads for Buildings and Other Structures, ASCE, New York.

[4] Standards Australia (2011) AS/NZS 1170.2: 2011 Structural design actionsPart 2: Wind actions, Standards Australia, NSW.

[5] S. Panwar, Y. Kaushik, A. Singh, and N. Sharma, "Structural analysis and design of steel transmission tower in wind zones II and IV: a comparative study," Int J Eng Technol Manag Appl Sci, vol. 4, no. 5, pp. 168–177, 2016.

[6] S. T. Chyrmang, "Analysis of Transmission Tower," Int. Res. J. Eng. Technol., vol. 7, no. 8, pp. 507–512, 2020.

[7] A. K. Pal, M. Suneel, and P. V. Rambabu, "Comparative analysis of transmission tower using xx and xbx bracing systems in different wind zones," Int. J. Recent Technol. Eng., vol. 8, no. 1, pp. 56–61, 2019.

[8] ANSYS Fluent Software | CFD Simulation. (2019). Retrieved September 4, 2019, from https://www. ansys.com/ products/ fluids/ansys-fluent Inc. ANSYS. (2012). ANSYS FLUENT theory guide V14.5. ANSYS Fluent Solver Theory Guide.

[9] IS 802 (Part l/Sec 1) :1995, use of structural steel in overhead transmission line towers code of practice.

[10] Patankar, S. V., Numerical Heat Transfer and Fluid Flow McGraw-Hill (1980)